

RESEARCH LETTER

10.1002/2014GL062938

Key Points:

- Observed diurnal and annual cycles of the 10 m wind misrepresented by reanalyses
- Wind erosion is strongly underestimated with all reanalyses
- Impact on forecast and climate studies, soil erosion, and health issues

Supporting Information:

- Appendices SA–SG and Figures SA1–SG2

Correspondence to:

Y. Largeron,
yann.largeron@meteo.fr

Citation:

Largeron, Y., F. Guichard, D. Bouniol, F. Couvreux, L. Kergoat, and B. Marticorena (2015), Can we use surface wind fields from meteorological reanalyses for Sahelian dust emission simulations?, *Geophys. Res. Lett.*, 42, doi:10.1002/2014GL062938.

Received 22 DEC 2014

Accepted 5 MAR 2015

Accepted article online 10 MAR 2015

Can we use surface wind fields from meteorological reanalyses for Sahelian dust emission simulations?

Yann Largeron¹, Françoise Guichard¹, Dominique Bouniol¹, Fleur Couvreux¹, Laurent Kergoat², and Béatrice Marticorena³

¹Centre National de Recherches Meteorologiques, CNRM-GAME, CNRS, Toulouse, France, ²Géosciences Environnement Toulouse, CNRS-UPS-IRD, Toulouse, France, ³LISA, Universités Paris Est-Paris Diderot-Paris 7, Créteil, France

Abstract The Sahel is prone to intense soil erosion, and the dust emission flux is very sensitive to the surface wind speed. In this study, we use high-frequency observations acquired across the Sahel to assess the ability of three global reanalyses (ERA-interim, NCEP-CFSR and MERRA) to capture the observed surface wind events that are critical to wind erosion. ERA-Interim is shown to perform best. However, all three reanalyses present a too flat annual cycle, with important season-dependent biases: they overestimate the surface wind during dry season nights and underestimate it during spring and monsoon season days. More importantly, the strongest wind speeds, observed in the morning and during deep convective events, are systematically underestimated. As analyzed wind fields are one of the main inputs of many dust emission models, their too low fraction of high wind speeds will lead to major errors in dust emission simulations.

1. Introduction

Wind erosion over North Africa is responsible for 25 to 50% of the global emissions of mineral dust [Engelstaedter *et al.*, 2006]. These emissions affect the climate [Carslaw *et al.*, 2010] due to their radiative impact, which still remains a significant source of uncertainty in climate projections [Intergovernmental Panel on Climate Change, 2007, 2013].

In the Sahel, wind erosion is a crucial issue for people and the local economy, which heavily depends on agriculture [United Nations, 2012]. As upper soil layers contain most of the nutrients needed for plant growth, erosion lead to a significant midterm loss of soil fertility and productivity [Biellers *et al.*, 2002].

Wind erosion also generates strong dust emission [Rajot *et al.*, 2012]. Consequently, atmospheric concentrations of particulate matter less than 10 μm (PM_{10}) frequently reach very high values, up to several thousands of $\mu\text{g m}^{-3}$ [Ozer *et al.*, 2007; Marticorena *et al.*, 2010], far above the World Health Organization quality standards (daily mean less than 50 $\mu\text{g m}^{-3}$). High PM_{10} concentrations have numerous undesired consequences on human health [Pope *et al.*, 2002] and have been related to meningitis in the Sahel [Martiny and Chiapello, 2013].

Quantifying the amount of dust uplifted by the wind is therefore an issue of particular importance [Knippertz and Todd, 2012]. It has been shown that the dust emission flux varies with the cube of the surface friction velocity above a threshold which depends on soil surface characteristics [Marticorena and Bergametti, 1995].

In West Africa, dust emission events are mainly related to two meteorological processes leading to high surface wind speeds: turbulent mixing of the nocturnal low-level jet (LLJ) [Washington and Todd, 2005; Fiedler *et al.*, 2013] and gust fronts induced by convective cold pools [Flamant *et al.*, 2007; Marsham *et al.*, 2008; Rajot *et al.*, 2012; Marticorena *et al.*, 2010]. Typically, a significant fraction of the dust uplift occurs during isolated events which generate violent cold pool outflows caused by moist deep convection (cf. results from observations over the Sahel [Rajot, 2001; Abdourhamane Toure *et al.*, 2011] and Sahara [Marsham *et al.*, 2013a] or from a model [Heinold *et al.*, 2013]).

Meteorological reanalyses are well suited to capture synoptic-scale dynamical processes, but biases in surface wind speeds can be induced through conceptual limitations. First, because of their physical parameterizations, density currents resulting from deep convection enhance the surface wind speed [Charba, 1974; Goff, 1976; Houze and Betts, 1981] and are not parameterized in atmospheric models like those used for meteorological reanalyses. Second, their coarse resolution and time sampling is not well adapted to transient strong wind events occurring at the mesoscale and generating a large subgrid scale variability.

Several recent studies [Todd *et al.*, 2008; Knippertz *et al.*, 2009; Marsham *et al.*, 2011, 2013a; Fiedler *et al.*, 2013], based on cases studies, have indeed pointed out or suggested some misrepresentations of the wind in reanalyses. As dust emission fluxes are directly linked to the surface wind speed, they are particularly sensitive to the wind fields [Luo *et al.*, 2003; Schmechtig *et al.*, 2011]; the estimated fluxes can vary by a factor of 3 when using wind fields from different reanalyses [Menut, 2008]. These results lead to a growing concern on the use of reanalyses to simulate Sahelian dust emissions, but a systematic evaluation of this issue is still lacking.

In the meantime, meteorological reanalyses are more and more commonly used as input fields for dust emission simulations over North Africa [Tegen *et al.*, 2002; Gong *et al.*, 2003; Washington *et al.*, 2003; Huneus *et al.*, 2011; Pierre *et al.*, 2012; Doherty *et al.*, 2014; Ridley *et al.*, 2014; Albani *et al.*, 2014; Kim *et al.*, 2014], because they use a homogeneous forecasting system for long time periods (typically 30 to 50 years), making them the most suitable products for the purpose of long-term studies and simulations.

The present study investigates the ability of several reanalyses to represent the previously described processes, in order to point out potential deficiencies. To this purpose, several years of high-frequency wind observations acquired at different locations across the Sahel are used to examine the performances of three global reanalyses.

2. Data and Method

2.1. Data

We use the following reanalyses: ERA-Interim (European Re-Analysis) from the European Centre for Medium-Range Weather Forecasts (ECMWF) [Dee *et al.*, 2011]; NCEP-CFSR (National Centers for Environmental Prediction's Climate Forecast System Reanalysis) from the National Oceanic and Atmospheric Administration (NOAA) [Saha *et al.*, 2010]; MERRA (Modern Era Retrospective for Research and Applications) from the National Aeronautics and Space Administration [Rienecker *et al.*, 2011].

The 10 m wind speed is available every 3 h for ERA-Interim and every hour for NCEP-CFSR and MERRA. This time resolution allows to capture the LLJ breakdown which occurs in the morning. The spatial resolutions are about 80 km \times 80 km, 38 km \times 38 km, and 55 km \times 70 km for ERA-Interim, NCEP-CFSR, and MERRA, respectively (see supporting information (SI) Appendix SA, for more information).

We also use observations from the network of the African Monsoon Multidisciplinary Analyses (AMMA) program [Redelsperger *et al.*, 2006] and focus on four measurement sites chosen to sample the climatology of the surface wind speed in the Sahel, covering an area of about 1000 km \times 400 km (SI Figure SA1). These observations were collected over 5 years or more in Cinzana (Mali), 13.28°N, 5.93°W, at 2.3 m above ground, and Banizoumbou (Niger), 13.54°N, 2.66°E, at 6.5 m as part of the AMMA Sahelian Dust Transect (SDT) [Marticorena *et al.*, 2010]; Agoufou (Mali), 15.34°N, 1.48°W, and Bamba (Mali), 17.1°N, 1.4°W, at 3 m at both sites as part of the AMMA-Couplage de l'Atmosphère Tropicale et du Cycle Hydrologique (CATCH) network in Mali [Mougin *et al.*, 2009]. See more details in SI Appendix SA.

A 15 min average is applied to the observed wind speed time series acquired at higher frequency to match typical analysis time step. All wind speed measurements are extrapolated to 10 m assuming a logarithmic profile [Stull, 1987]. This accounts for a maximum bias of less than 0.5 m s⁻¹ in strongly stable cases (see SI Appendix SB). Following Lloyd *et al.* [1992], surface roughness lengths are estimated from the ratio of the wind speed to friction velocity measured using the eddy correlation technique at Agoufou and Bamba, where turbulence observations are available. Otherwise, we use values from ERA-Interim. Estimated annual-averaged surface roughness lengths are 0.001 m at the northern bare soil site of Bamba, 0.05 m at Agoufou, 0.18 m at Banizoumbou, and 0.23 m at the southwestern vegetated site of Cinzana.

2.2. Method

For comparison between observations and reanalyses, we use at each site the closest reanalysis grid point (results are similar with a distance-weighted interpolation of the four nearest grid points) and a 3-hourly subsampling of the 15 min running-average observed wind speeds time series. Since the wind in reanalysis is computed at a resolution of several tens of kilometers, a perfect match with local observation is not expected because local characteristics may impact the comparison with a large-scale model. Consequently, we limit our analysis to systematic biases emerging from comparisons at all the observational sites on long

time series. We analyze in particular statistics from diurnal to seasonal timescales with Taylor diagrams [Taylor, 2001], using daily mean wind speed and its 3-hourly fluctuations around the mean.

The wind speed probability density function (PDF) is investigated in order to evaluate the fraction of high wind speeds. Focus is put on convective events, detected using two complementary criteria. The first consists in defining the occurrence of convection when precipitation is locally recorded. The associated convective event is extended to the 30 min before the first rain and the 30 min following the last rain. The second is based on the satellite-based tracking of Mesoscale Convective Systems (MCSs) of Folleau and Roca [2013]. The algorithm operates with infrared images to track MCSs and provides estimations of MCSs occurrence over the observational sites every 30 min. Both criteria lead to minor differences in the detection of convective events, which implies that most of the tracked MCSs are precipitating and conversely that local precipitation is mainly provided by MCSs, consistently with the findings of Laurent *et al.* [1998]. In the following, a convective event is defined whenever one of the two criteria is met.

Finally, we attempt to quantify the influence of the wind fields on the dust emission fluxes and compute a Dust Uplift Potential (DUP) as proposed by Marsham *et al.* [2011]. DUP is proportional to the dust emission flux if the effects of stability, soil moisture, and roughness variations are neglected:

$$\text{DUP} = U^3 \left(1 + \frac{U_t}{U} \right) \left(1 - \frac{U_t^2}{U^2} \right), \quad (1)$$

where U is the 10 m surface wind speed and U_t the corresponding threshold at 10 m.

Accumulated DUP (hereafter $\overline{\text{DUP}}$) is further computed by integrating instantaneous DUP over a whole year.

3. Evaluation of Reanalyses at Different Timescales

3.1. Annual Cycle and Synoptic Timescale

According to observations (Figure 1a for Banizoumbou and Figure SC1 in Appendix SC for the other sites), the surface wind speed over the Sahelian belt is lower during the dry season (November to February, day of year 305 to 365 and 1 to 60), increases in spring (April, May, and June, day of year 60 to 182) until reaching its maximum at the beginning of July (around day of year 182). Then, it slowly decreases during the monsoon (May to September, day of year 121 to 273) and later to reach a late autumn minimum (around day of year 305). This annual cycle is consistent with the results of Lothon *et al.* [2008] and Guichard *et al.* [2009] and follows the well-known Sahelian climatological alternance between the dry and northeasterly Harmattan wind and the moist and southwesterly monsoon wind [Hastenrath *et al.*, 1991; Thorncroft *et al.*, 2011].

The three reanalyses display rather different features of this annual cycle with mean annual biases of 0.27 m s^{-1} for ERA-Interim, 0.70 m s^{-1} for MERRA, and -0.62 m s^{-1} for NCEP-CFSR, with the estimated values of surface roughness lengths. These mean annual biases involve much larger season-dependent biases that are qualitatively shared by the three reanalyses.

During the monsoon season, observed high-frequency winds (Figure 1b) exhibit large day-to-day fluctuations, and a few sporadic very high 10 m wind speeds related to the occurrence of convective events. The three reanalyses are close to each other and follow the observed synoptic fluctuations. However, they systematically miss the high wind speeds associated with deep convection. This increase of the wind speed due to convective events is still evident from the 3 h subsampled observations (yellow curve in Figure 1), which points to the misrepresentation of convectively driven high wind speeds in the reanalyses, beyond their too coarse time sampling. In the three reanalyses, the wind speed always tends to be lower than observed (see SI Appendix SD and Figure SD1 for statistics). This highlights uncertainties in the processes controlling wind speed that could involve the representation of the large-scale dynamics [Marsham *et al.*, 2011, 2013b] or the daytime boundary layer mixing in the reanalyses. NCEP-CFSR behaves worst and largely underestimates wind speeds, which is consistent with previous studies [Menut, 2008; Koren and Kaufman, 2004].

During the dry season, observations (Figure 1c) indicate a strong influence of the diurnal cycle on the 10 m wind speed. It is very low during nighttime, sharply increases in the morning, and then slowly decreases throughout the afternoon. In MERRA and ERA-Interim, the wind speed tends to be significantly stronger than observed (Figures 1a and 1c). This seasonal bias arises from a systematic overestimation of the nighttime wind speed which is also shared by NCEP-CFSR, as discussed in section (3.2).

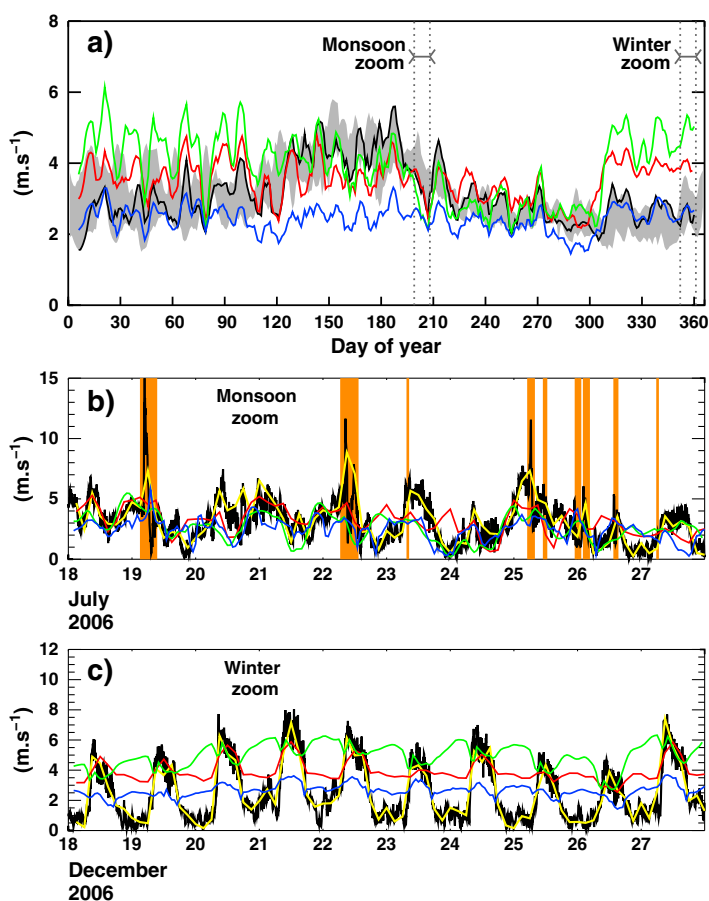


Figure 1. Time series of the 10 m wind speed in 2006 at Banizoumbou. (a) Annual cycle of the 5 day running mean. Vertical dashed lines indicate when the zoomed time series of Figures 1b and 1c are taken. Nine day time series in the (b) monsoon and (c) dry seasons. Black: 5 min observations; red: ERA-Interim; blue: NCEP-CFSR; green: MERRA; yellow: 3-hourly sampling of a 15 min running mean of the observations. Orange: occurrence of MCSs. The grey shading in Figure 1a shows the range of minimum and maximum observed values over 2006–2011.

The combination of these two season-dependent biases lead to an unrealistically flat amplitude of the annual cycle of the surface wind speed, in the three reanalyses. It is much too weak in NCEP-CFSR (2.37 m s^{-1} against 4.30 m s^{-1} for the observations on average over the four sites). MERRA and ERA-Interim present a larger amplitude of the annual cycle, with a progressive decrease of the surface wind speed during the monsoon, as observed, but still a too smooth annual cycle (with an annual amplitude of 4.10 and 3.48 m s^{-1} , respectively).

3.2. Diurnal Cycle

During the dry season, low-level dynamics are strongly controlled by boundary layer processes and nighttime surface wind speeds are very low at all sites (Figures 2c, 2f, 2i, and 2l), due to the atmospheric stability that inhibits turbulence [Guichard *et al.*, 2009; Bain *et al.*, 2010]. In all reanalyses, nighttime 10 m wind speeds are systematically overestimated (Figures 1c, 2c, 2f, 2i, and 2l), which accounts for the strong positive biases in ERA-Interim and MERRA during the dry season (Figure 1a). MERRA wind speeds are so unrealistically high during winter nights that the diurnal cycle is almost reversed (Figure 1c). NCEP-CFSR is characterized by an unrealistically weak diurnal amplitude, which leads to a reasonable estimation of the diurnal-averaged wind speed (Figure 1a) via two compensating errors: a too high wind speed at night and a too low wind speed during the day. The nighttime overestimation of wind speed, found in all reanalyses, is consistent with an overestimation of the turbulent diffusion in the nighttime dry stable surface layer. Nocturnal diffusion is indeed artificially enhanced in models for practical considerations [Sandu *et al.*, 2013]. This induces a too strong mixing with the LLJ often present at a typical altitude of 300 m above the ground [Fiedler *et al.*, 2013] and therefore leads to an overestimation of the surface wind speed.

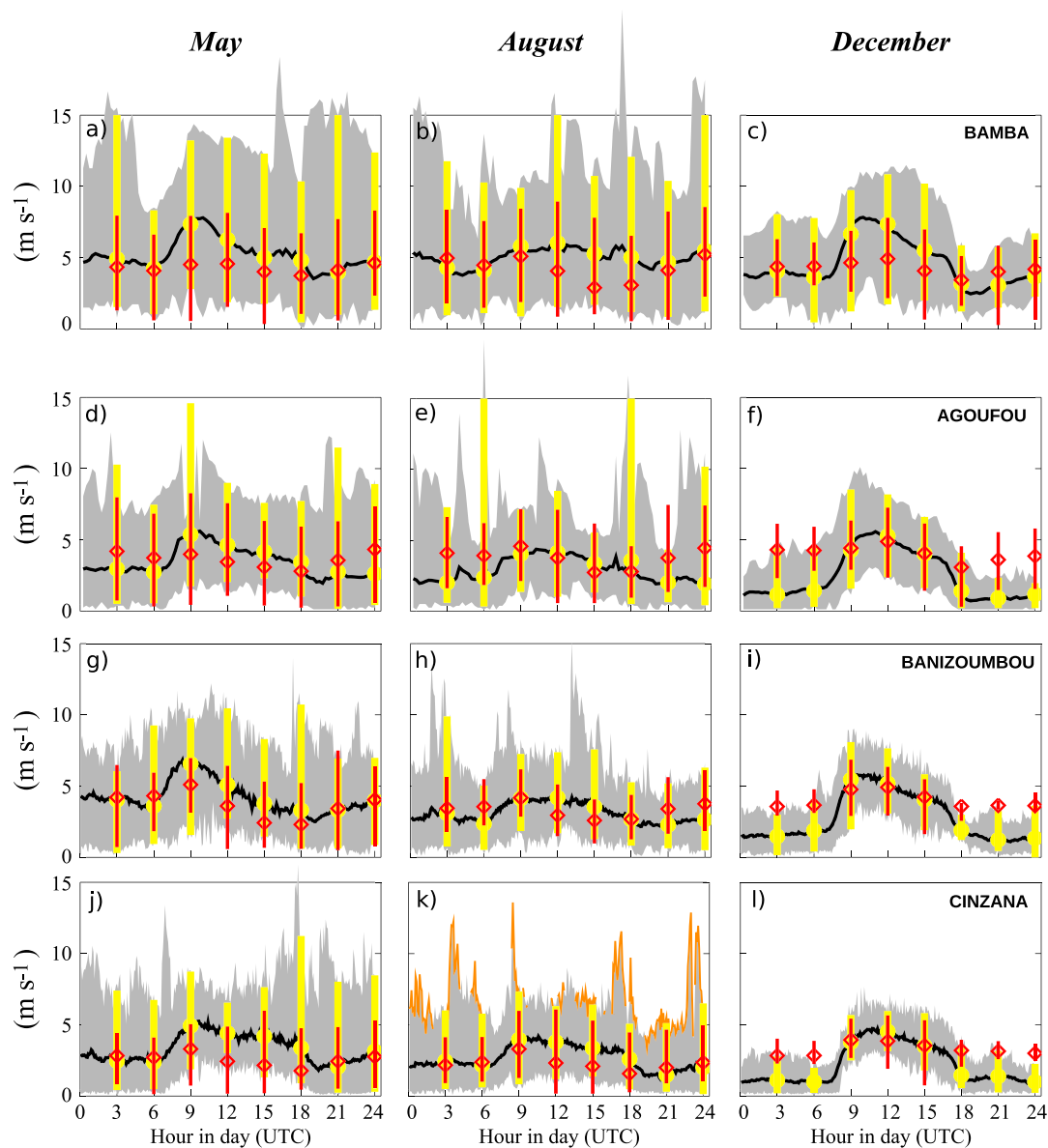


Figure 2. Monthly mean diurnal cycles of mean and extreme 10 m wind speeds at four sites for (a, d, g, and j) May, (b, e, h, and k) August, and (c, f, i, and l) December 2006. Observational (δt : 15 min running mean) mean (black) and extremes (grey shading). ERA-Interim (red) mean (diamonds) and extremes (bars) and 3 h sampled observed (yellow) mean (circles) and extremes (bars). Wind maxima associated with convective events are shown in orange in Figure 2k.

In winter and spring, the monthly averaged diurnal cycle (Figures 2a, 2d, 2g, 2j, 2c, 2f, 2i, and 2l) exhibits a well-marked maximum of the wind in the morning (around 9 h) corresponding to the turbulent mixing of the LLJ by boundary layer dry convection [Parker *et al.*, 2005]. In the reanalyses, the morning increase of the 10 m wind speed is always weaker at all sites (see SI Appendix SE for MERRA and NCEP-CFSR). This suggests an underestimation of the LLJ core wind speed, as noted by Fiedler *et al.* [2013] for ERA-Interim, and/or some misrepresentation of the mixing rate.

Other sporadic wind maxima related with convective events occur, during the spring and monsoon months, as illustrated by the minimum-maximum envelope (in Figure 2; this envelope is indicated by grey shading and convection by the orange line). These extreme winds associated with convection are totally missing in reanalyses.

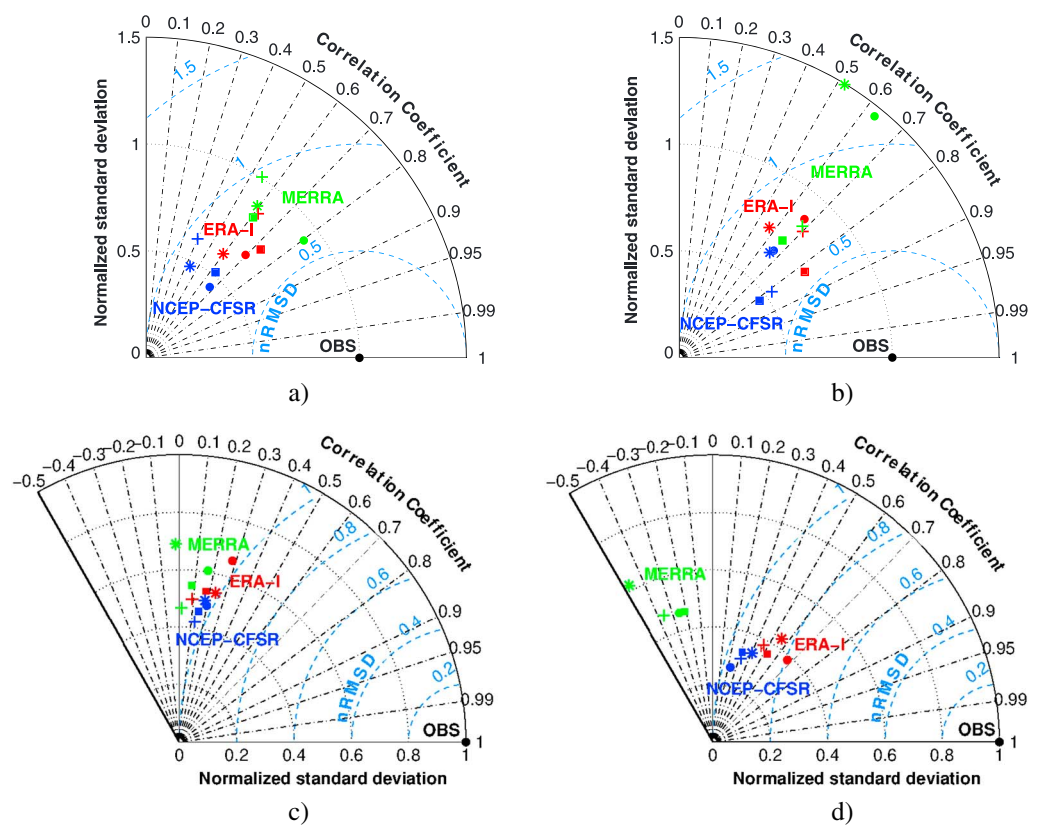


Figure 3. Normalized Taylor diagrams synthesizing normalized standard deviations ($\bar{\sigma}_{rea}$), correlation coefficients, and normalized root-mean-square deviations (nRMSD) of the 10 m wind speed from reanalyses compared to observations for the 2006–2011 period. The observational references are shown with the black dots. Red: ERA-Interim; blue: NCEP-CFSR; green: MERRA; circles: Banizoumbou; stars: Cinzana; crosses: Agoufou; squares: Bamba; for the daily mean wind speeds during the (a) monsoon season (from May to September) and the (b) dry season (from November to February); (c and d) same as Figures 3a and 3b but for the 3-hourly fluctuations around the daily mean wind speed.

In reanalyses, whatever the season, the diurnal amplitude and the monthly variability tend to be underestimated. This mainly results from the underestimation of the daytime wind speed during the monsoon season, and from the overestimation of the nighttime wind speed during the dry season.

4. Statistical Analysis and Dust Uplift Potential

4.1. Taylor Diagrams

A comparison of statistics is made on Taylor diagrams (Figure 3). During both seasons, synoptic and intraseasonal fluctuations are captured by the three reanalyses. Correlation coefficients between observed and analyzed daily mean wind are higher than 0.5–0.6 (Figures 3a and 3b), but this is associated with a too low standard deviation in ERA-Interim and NCEP-CFSR (underestimated by 13 to 54%). Mean biases of the daily mean wind speed are significant in the three reanalyses, up to 2 m s^{-1} in dry season and -2 m s^{-1} during monsoon (see SI Appendix SD and Figure SD1 (right column)). The performance of the reanalyses drops sharply at subdaily time scale (Figures 3c and 3d), leading to higher normalized root-mean-square deviations (nRMSD) and smaller correlation coefficients. This means that the misrepresentation largely comes from biases in the diurnal cycle.

Of the three reanalyses, ERA-Interim performs best in terms of timing (best correlation coefficient) and representation of the diurnal cycle. It also gives reasonable but slightly underestimated standard deviations. MERRA gives good estimates of the standard deviation but displays a strong positive bias and a negative correlation with observation at subdaily timescales in dry season. NCEP-CFSR has a reasonable correlation with observation at synoptic timescale but much too weak variability and diurnal cycle amplitude.

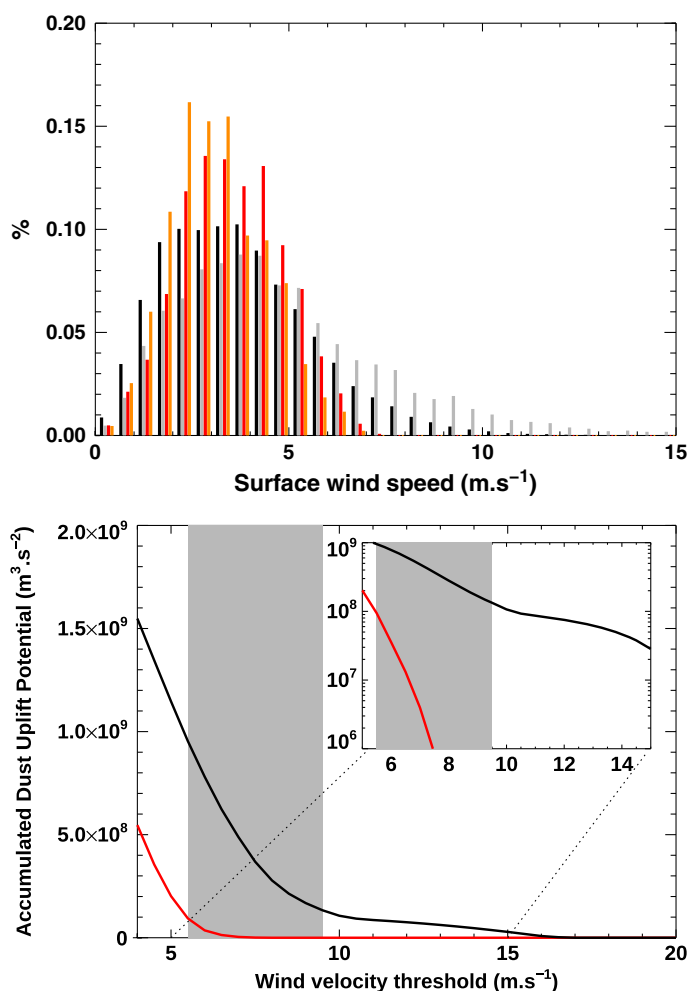


Figure 4. (top) Probability density functions (PDF) of 10 m wind speed in Banizoumbou during the monsoon season (from May to September) of 2006: observations (black) and ERA-Interim (red); or during convective events only: observations (grey) and ERA-Interim (orange). (bottom) Accumulated Dust Uplift Potential DUP in Banizoumbou over the whole year 2006 (red: ERA-Interim; black: observations). Grey shading: typical range of values of U_t . Inset: zoom over the wind velocity range delimited by the dashed lines, with \overline{DUP} in log scale.

4.2. Wind Speed Distribution

The 10 m wind speed PDF is computed for the whole monsoon period, during which most convective events happen (cf. Figure 4 for Banizoumbou, SI Appendix SF for the other sites in 2006, and Appendix SG for other years).

Compared to observations (black bars in Figure 4 (top)), the ERA-Interim PDF (red bars) is shifted toward lower values and contains a significantly smaller fraction of high wind speeds (with no value above 7 m s^{-1} , whereas observations show values up to 20 m s^{-1}). This is worst if the comparison is restricted to convective events: the observed wind PDF grey bars then shows a higher fraction of wind between 7 m s^{-1} and 20 m s^{-1} than for the whole monsoon period. This highlights that the highest wind speed values are mostly related to deep convection. On the opposite, in ERA-Interim, the PDFs for the whole monsoon and during convective events only are very similar (red and orange bars, respectively); and the differences between the observed PDF and the ERA-Interim PDF is significantly increased during convective events. This demonstrates that the frequency of high wind speed is significantly underestimated and implies that deep convective events are missing in ERA-Interim, consistently with *Marshall et al.* [2011].

4.3. Dust Uplift Potential

\overline{DUP} (equation (1)) is computed over the whole year of 2006 as a function of the threshold velocity U_t (Figure 4, bottom).

The threshold U_t actually depends on local soil characteristics. A quantification of the local roughness length z_0 (cf. section 2) and of the threshold U_t [Abdourhamane Toure *et al.*, 2011; Pierre *et al.*, 2014] for the observational site shows that U_t varies from 5.5 to 9.5 m s^{-1} , which is consistent with Cowie *et al.* [2014]. When using a typical value of $U_t = 7 \text{ m s}^{-1}$, the computation from ERA-Interim wind speeds leads to an underestimation of the DUP by 2 orders of magnitude. For the lower value of $U_t = 5.5 \text{ m s}^{-1}$, the DUP is underestimated by a factor 10 relative to ERA-Interim. For $U_t > 7.5 \text{ m s}^{-1}$, computation from ERA-Interim gives no DUP at all, against significant values from observations.

5. Conclusion

The present study provides, for the first time, a systematic evaluation of several meteorological reanalyses with high-frequency long-term observations. We used surface wind observations collected across the Sahelian belt to investigate the ability of three reanalyses (ERA-Interim, MERRA, and NCEP-CFSR) to reproduce observations.

Of the three reanalyses, ERA-Interim performs best in terms of representation of the annual and diurnal cycles and synoptic and intraseasonal fluctuations of surface wind speed. All reanalyses nevertheless miss some key features of the climatology and of the mesoscale dynamics of the surface wind speed. Results from all sites point to the same main issues:

1. The amplitude of the annual cycle is unrealistically flat in all reanalyses, due to the combination of a positive bias during the dry season and a negative bias during the monsoon season.
2. During the dry season, the amplitude of the diurnal cycle is highly underestimated, mainly because the nighttime wind speed is systematically overestimated. This could be due to the artificially enhanced turbulent diffusion in nighttime stable layers [Sandu *et al.*, 2013]. In MERRA, the nighttime wind speed is so unrealistically high that the diurnal cycle appears reversed.
3. During the spring and monsoon seasons, the amplitude of the diurnal cycle is underestimated, due to the underestimation of the daytime wind speed, especially in the morning in spring, when the nocturnal low-level jet is mixed downward by boundary layer convection, via the mechanisms discussed by Hourdin *et al.* [2014] and Fiedler *et al.* [2013].
4. Reanalyses are missing major features of the mesoscale dynamics, and especially the increase of the surface wind speed associated with deep convection. This phenomenon appears in all observational data sets but is totally absent in the reanalyses, consistently with the findings of previous work on more limited data [Knippertz *et al.*, 2009; Marsham *et al.*, 2011; Heinold *et al.*, 2013].

These two last points are responsible for large differences in the probability density functions of surface wind speeds, especially at extreme values ($> 7 \text{ m s}^{-1}$), which is critical in terms of dust emissions. Indeed, quantifications of the DUP [Marsham *et al.*, 2011] show that the use of the ERA-Interim 10 m wind speed for that purpose can lead to an underestimation of the DUP by 1 or 2 orders of magnitude.

Therefore, if one wants to use these reanalyses fields as forcing for dust emission models in the Sahel, it appears crucial to first apply a correction to the winds in order to take into account the effect of convection on wind-driven dust emissions. The magnitude of the LLJ should also be corrected since the wind associated to this pattern often reaches the uplift threshold in the northern Sahel. Moreover, this study highlights some processes that are missing in the atmospheric models used for meteorological reanalyses, and long-term efforts are and should be undertaken to improve the representation of the surface wind dynamics at turbulent and mesoscales.

References

- Abdourhamane Toure, A., J. L. Rajot, Z. Garba, B. Marticorena, C. Petit, and D. Sebag (2011), Impact of very low crop residues cover on wind erosion in the Sahel, *Catena*, 85(3), 205–214, doi:10.1016/j.catena.2011.01.002.
- Albani, S., N. M. Mahowald, A. T. Perry, R. A. Scanza, C. S. Zender, N. G. Heavens, V. Maggi, J. F. Kok, and B. L. Otto-Bliesner (2014), Improved dust representation in the Community Atmosphere Model, *J. Adv. Model. Earth Syst.*, 6, 541–570, doi:10.1002/2013MS000279.
- Bain, C., D. J. Parker, C. M. Taylor, L. Kergoat, and F. Guichard (2010), Observations of the nocturnal boundary layer associated with the West African monsoon, *Mon. Weather Rev.*, 138(8), 3142–3156, doi:10.1175/2010MWR3287.1.
- Bielders, C. L., J.-L. Rajot, and M. Amadou (2002), Transport of soil and nutrients by wind in bush fallow land and traditionally managed cultivated fields in the Sahel, *Geoderma*, 109(1), 19–39, doi:10.1016/S0016-7061(02)00138-6.
- Carlsaw, K., O. Boucher, D. Spracklen, G. Mann, J. Rae, S. Woodward, and M. Kulmala (2010), A review of natural aerosol interactions and feedbacks within the Earth system, *Atmos. Chem. Phys.*, 10(4), 1701–1737, doi:10.5194/acp-10-1701-2010.

Acknowledgments

This work has been done in the framework of the CAVIARS project from the French national research agency (ANR). Support from ANR CAVIARS, grant ANR-12-SENV-0007-01, is acknowledged. The authors would like to thank Christel Bouet and Caroline Pierre for help and discussions. The authors also thank F. Timouk, J.L. Rajot, B. Chatenet, and all the technicians who helped in collecting the SDT and AMMA-CATCH data in Niger and Mali. The ERA-Interim data were retrieved from the ECMWF MARS archive, available from <http://www.ecmwf.int/>. NCEP/CFSR data were retrieved from the NOAA National Operational Model Archive and Distribution System (NOMADS) at NCDC (<http://cfs.ncep.noaa.gov/cfsr/>). Authors also acknowledge the Global Modeling and Assimilation Office (GMAO) and the GES DISC for the dissemination of MERRA data, available from <http://gmao.gsfc.nasa.gov/research/merra/>.

The Editor thanks John Marsham and an anonymous reviewer for their assistance in evaluating this paper.

- Charba, J. (1974), Application of gravity current model to analysis of squall-line gust front, *Mon. Weather Rev.*, *102*(2), 140–156, doi:10.1175/1520-0493(1974)1020140:AOGCMT2.0.CO;2.
- Cowie, S., P. Knippertz, and J. Marsham (2014), A climatology of dust emission events from northern Africa using long-term surface observations, *Atmos. Chem. Phys.*, *14*, 8579–8597, doi:10.5194/acp-14-8579-2014.
- Dee, D., et al. (2011), The ERA-Interim reanalysis: Configuration and performance of the data assimilation system, *Q. J. R. Meteorol. Soc.*, *137*(656), 553–597, doi:10.1002/qj.828.
- Doherty, O. M., N. Riemer, and S. Hameed (2014), Role of the convergence zone over West Africa in controlling Saharan mineral dust load and transport in the boreal summer, *Tellus B*, *66*, 23191, doi:10.3402/tellusb.v66.23191.
- Engelstaedter, S., I. Tegen, and R. Washington (2006), North African dust emissions and transport, *Earth Sci. Rev.*, *79*(1), 73–100, doi:10.1016/j.earscirev.2006.06.004.
- Fiedler, S., K. Schepanski, B. Heinold, P. Knippertz, and I. Tegen (2013), Climatology of nocturnal low-level jets over North Africa and implications for modeling mineral dust emission, *J. Geophys. Res. Atmos.*, *118*, 6100–6121, doi:10.1002/jgrd.50394.
- Fioleau, T., and R. Roca (2013), An algorithm for the detection and tracking of tropical mesoscale convective systems using infrared images from geostationary satellite, *IEEE Trans. Geosci. Remote Sens.*, *51*(7), 4302–4315, doi:10.1109/TGRS.2012.2227762.
- Flamant, C., J.-P. Chaboureau, D. J. Parker, C. M. Taylor, J.-P. Cammas, O. Bock, F. Timouk, and J. Pelon (2007), Airborne observations of the impact of a convective system on the planetary boundary layer thermodynamics and aerosol distribution in the inter-tropical discontinuity region of the West African monsoon, *Q. J. R. Meteorol. Soc.*, *133*(626), 1175–1189, doi:10.1002/qj.97.
- Goff, R. C. (1976), Vertical structure of thunderstorm outflows, *Mon. Weather Rev.*, *104*(11), 1429–1440, doi:10.1175/1520-0493(1976)1041429:VSOTO2.0.CO;2.
- Gong, S., X. Zhang, T. Zhao, I. McKendry, D. Jaffe, and N. Lu (2003), Characterization of soil dust aerosol in China and its transport and distribution during 2001 ACE-Asia: 2. Model simulation and validation, *J. Geophys. Res.*, *108*(D9), 4262, doi:10.1029/2002JD002633.
- Guichard, F., L. Kergoat, E. Mougou, F. Timouk, F. Baup, P. Hiernaux, and F. Lavenu (2009), Surface thermodynamics and radiative budget in the Sahelian Gourma: Seasonal and diurnal cycles, *J. Hydrol.*, *375*(1), 161–177, doi:10.1016/j.jhydrol.2008.09.007.
- Hastenrath, S., et al. (1991), *Climate Dynamics of the Tropics*, Kluwer Acad., Dordrecht, Netherlands.
- Heinold, B., P. Knippertz, J. Marsham, S. Fiedler, N. Dixon, K. Schepanski, B. Laurent, and I. Tegen (2013), The role of deep convection and nocturnal low-level jets for dust emission in summertime West Africa: Estimates from convection-permitting simulations, *J. Geophys. Res. Atmos.*, *118*, 4385–4400, doi:10.1002/jgrd.50402.
- Hourdin, F., M. Gueye, B. Diallo, J.-L. Dufresne, L. Menut, B. Marticorena, G. Siour, and F. Guichard (2014), Parametrization of convective transport in the boundary layer and its impact on the representation of diurnal cycle of wind and dust emissions, *Atmos. Chem. Phys. Discuss.*, *14*(19), 27,425–27,458, doi:10.5194/acpd-14-27425-2014.
- Houze, R. A., and A. K. Betts (1981), Convection in GATE, *Rev. Geophys.*, *19*(4), 541–576, doi:10.1029/RG019i004p00541.
- Huneus, N., et al. (2011), Global dust model intercomparison in AEROCOM phase I, *Atmos. Chem. Phys.*, *11*(15), 7781–7816, doi:10.5194/acpd-10-23781-2010.
- Kim, D., et al. (2014), Sources, sinks, and transatlantic transport of North African dust aerosol: A multimodel analysis and comparison with remote sensing data, *J. Geophys. Res. Atmos.*, *119*, 6259–6277, doi:10.1002/2013JD021099.
- Knippertz, P., and M. C. Todd (2012), Mineral dust aerosols over the Sahara: Meteorological controls on emission and transport and implications for modeling, *Rev. Geophys.*, *50*, RG1007, doi:10.1029/2011RG000362.
- Knippertz, P., et al. (2009), Dust mobilization and transport in the northern Sahara during SAMUM 2006—A meteorological overview, *Tellus*, *61*(1), 12–31, doi:10.1111/j.1600-0889.2008.00380.x.
- Koren, I., and Y. J. Kaufman (2004), Direct wind measurements of Saharan dust events from Terra and Aqua satellites, *Geophys. Res. Lett.*, *31*, L06122, doi:10.1029/2003GL019338.
- Laurent, H., N. D'Amato, and T. Lebel (1998), How important is the contribution of the mesoscale convective complexes to the Sahelian rainfall?, *Phys. Chem. Earth*, *23*(5), 629–633, doi:10.1016/S0079-1946(98)00099-8.
- Lloyd, C., J. Gash, and M. Sivakumar (1992), Derivation of the aerodynamic roughness parameters for a Sahelian savannah site using the eddy correlation technique, *Boundary Layer Meteorol.*, *58*(3), 261–271, doi:10.1007/BF02033827.
- Lothon, M., F. Saïd, F. Lohou, and B. Campistron (2008), Observation of the diurnal cycle in the low troposphere of West Africa, *Mon. Weather Rev.*, *136*(9), 3477–3500, doi:10.1175/2008MWR2427.1.
- Luo, C., N. M. Mahowald, and J. Del Corral (2003), Sensitivity study of meteorological parameters on mineral aerosol mobilization, transport, and distribution, *J. Geophys. Res.*, *108*(D15), 4447, doi:10.1029/2003JD003483.
- Marsham, J. H., D. J. Parker, C. M. Grams, C. M. Taylor, and J. M. Haywood (2008), Uplift of Saharan dust south of the intertropical discontinuity, *J. Geophys. Res.*, *113*, D21102, doi:10.1029/2008JD009844.
- Marsham, J. H., P. Knippertz, N. S. Dixon, D. J. Parker, and G. Lister (2011), The importance of the representation of deep convection for modeled dust-generating winds over West Africa during summer, *Geophys. Res. Lett.*, *38*, L16803, doi:10.1029/2011GL048368.
- Marsham, J. H., et al. (2013a), Meteorology and dust in the central Sahara: Observations from Fennec supersite-1 during the June 2011 Intensive Observation Period, *J. Geophys. Res. Atmos.*, *118*, 4069–4089, doi:10.1002/jgrd.50211.
- Marsham, J. H., N. S. Dixon, L. Garcia-Carreras, G. Lister, D. J. Parker, P. Knippertz, and C. E. Birch (2013b), The role of moist convection in the West African monsoon system: Insights from continental-scale convection-permitting simulations, *Geophys. Res. Lett.*, *40*(9), 1843–1849, doi:10.1002/grl.50347.
- Marticorena, B., and G. Bergametti (1995), Modeling the atmospheric dust cycle: 1. Design of a soil-derived dust emission scheme, *J. Geophys. Res.*, *100*(D8), 16,415–16,430, doi:10.1029/95JD00690.
- Marticorena, B., B. Chatenet, J.-L. Rajot, S. Traoré, M. Coulibaly, A. Diallo, I. Koné, A. Maman, T. NDiaye, and A. Zakou (2010), Temporal variability of mineral dust concentrations over West Africa: Analyses of a pluriannual monitoring from the AMMA Sahelian Dust Transect, *Atmos. Chem. Phys.*, *10*(18), 8899–8915, doi:10.5194/acp-10-8899-2010.
- Martiny, N., and I. Chiapello (2013), Assessments for the impact of mineral dust on the meningitis incidence in West Africa, *Atmos. Environ.*, *70*, 245–253, doi:10.1016/j.atmosenv.2013.01.016.
- Menut, L. (2008), Sensitivity of hourly Saharan dust emissions to NCEP and ECMWF modeled wind speed, *J. Geophys. Res.*, *113*, D16201, doi:10.1029/2007JD009522.
- Mougou, E., et al. (2009), The AMMA-CATCH Gourma observatory site in Mali: Relating climatic variations to changes in vegetation, surface hydrology, fluxes and natural resources, *J. Hydrol.*, *375*(1), 14–33, doi:10.1016/j.jhydrol.2009.06.045.
- Ozer, P., M. B. O. M. Laghdaf, S. O. M. Lemine, and J. Gassani (2007), Estimation of air quality degradation due to Saharan dust at Nouakchott, Mauritania, from horizontal visibility data, *Water Air Soil Pollut.*, *178*(1–4), 79–87, doi:10.1007/s11270-006-9152-8.
- Parker, D., R. Burton, A. Diongue-Niang, R. Ellis, M. Felton, C. Taylor, C. Thorncroft, P. Bessemoulin, and A. Tompkins (2005), The diurnal cycle of the West African monsoon circulation, *Q. J. R. Meteorol. Soc.*, *131*(611), 2839–2860, doi:10.1256/qj.04.52.

- Pierre, C., G. Bergametti, B. Marticorena, E. Mougou, C. Bouet, and C. Schmechtig (2012), Impact of vegetation and soil moisture seasonal dynamics on dust emissions over the Sahel, *J. Geophys. Res.*, *117*, D06114, doi:10.1029/2011JD016950.
- Pierre, C., G. Bergametti, B. Marticorena, A. Abdourhamane Toure, J. L. Rajot, and L. Kergoat (2014), Modeling wind erosion flux and its seasonality from a cultivated Sahelian surface: A case study in Niger, *Catena*, *122*, 61–71, doi:10.1016/j.catena.2014.06.006.
- Pope, C. A., R. T. Burnett, M. J. Thun, E. E. Calle, D. Krewski, K. Ito, and G. D. Thurston (2002), Lung cancer, cardiopulmonary mortality, and long-term exposure to fine particulate air pollution, *Jama*, *287*(9), 1132–1141, doi:10.1001/jama.287.9.1132.
- Rajot, J.-L. (2001), Wind blown sediment mass budget of Sahelian village land units in Niger, *Bull. Soc. Geol. Fr.*, *172*(5), 523–531, doi:10.2113/172.5.523.
- Rajot, J.-L., A. Abdourhamane Touré, K. Desboeufs, P. Formenti, B. Marticorena, and M. Sow (2012), Le cycle des aérosols terrigènes au Sahel: Ce qu'AMMA nous a appris, *La Météorologie, Spécial AMMA*, doi:10.4267/2042/48130.
- Redelsperger, J.-L., C. D. Thorncroft, A. Diedhiou, T. Lebel, D. J. Parker, and J. Polcher (2006), African monsoon multidisciplinary analysis: An international research project and field campaign, *Bull. Am. Meteorol. Soc.*, *87*(12), 1739–1746, doi:10.1175/BAMS-87-12-1739.
- Ridley, D. A., C. L. Heald, and J. M. Prospero (2014), What controls the recent changes in African mineral dust aerosol across the Atlantic?, *Atmos. Chem. Phys.*, *14*(11), 5735–5747, doi:10.5194/acp-14-5735-2014.
- Rienecker, M. M., et al. (2011), MERRA: NASA's Modern-Era Retrospective Analysis for Research and Applications, *J. Clim.*, *24*(14), 3624–3648, doi:10.1175/JCLI-D-11-00015.1.
- Saha, S., et al. (2010), The NCEP climate forecast system reanalysis, *Bull. Am. Meteorol. Soc.*, *91*(8), 1015–1057, doi:10.1175/2010BAMS3001.1.
- Sandu, I., A. Beljaars, P. Bechtold, T. Mauritsen, and G. Balsamo (2013), Why is it so difficult to represent stably stratified conditions in Numerical Weather Prediction (NWP) models?, *J. Adv. Model. Earth Syst.*, *5*(2), 117–133, doi:10.1002/jame.20013.
- Schmechtig, C., B. Marticorena, B. Chatenet, G. Bergametti, J.-L. Rajot, and A. Coman (2011), Simulation of the mineral dust content over Western Africa from the event to the annual scale with the CHIMERE-DUST model, *Atmos. Chem. Phys.*, *11*(14), 7185–7207, doi:10.5194/acp-11-7185-2011.
- Intergovernmental Panel on Climate Change (2007), *Climate Change 2007: The Physical Science Basis. Contribution of Working Group I to the Fourth Assessment Report of the Intergovernmental Panel on Climate Change*, edited by S. Solomon et al., Cambridge Univ. Press, Cambridge, U. K., and New York.
- Intergovernmental Panel on Climate Change (2013), *Climate Change 2013: The Physical Science Basis. Contribution of Working Group I to the Fifth Assessment Report of the Intergovernmental Panel on Climate Change*, edited by T. F. Stocker et al., Cambridge Univ. Press, Cambridge, U. K., and New York.
- Stull, R. B. (1987), *An Introduction to Boundary Layer Meteorology*, vol. 666, Kluwer Acad., Dordrecht, Netherlands.
- Taylor, K. E. (2001), Summarizing multiple aspects of model performance in a single diagram, *J. Geophys. Res.*, *106*(D7), 7183–7192, doi:10.1029/2000JD900719.
- Tegen, I., S. P. Harrison, K. Kohfeld, I. C. Prentice, M. Coe, and M. Heimann (2002), Impact of vegetation and preferential source areas on global dust aerosol: Results from a model study, *J. Geophys. Res.*, *107*(D21), 4576, doi:10.1029/2001JD000963.
- Thorncroft, C. D., H. Nguyen, C. Zhang, and P. Peyrillé (2011), Annual cycle of the West African monsoon: Regional circulations and associated water vapour transport, *Q. J. R. Meteorol. Soc.*, *137*(654), 129–147, doi:10.1002/qj.728.
- Todd, M. C., R. Washington, S. Raghavan, G. Lizcano, and P. Knippertz (2008), Regional model simulations of the Bodélé low-level jet of northern Chad during the Bodélé Dust Experiment (BoDEx 2005), *J. Clim.*, *21*(5), 995–1012, doi:10.1175/2007JCLI1766.1.
- United Nations (2012), World population prospects, the 2012 revision.
- Washington, R., and M. C. Todd (2005), Atmospheric controls on mineral dust emission from the Bodélé depression, Chad: The role of the low level jet, *Geophys. Res. Lett.*, *32*, L17701, doi:10.1029/2005GL023597.
- Washington, R., M. Todd, N. J. Middleton, and A. S. Goudie (2003), Dust-storm source areas determined by the total ozone monitoring spectrometer and surface observations, *Ann. Assoc. Am. Geogr.*, *93*(2), 297–313, doi:10.1111/1467-8306.9302003.